

Hydrogen Bonding of CHCl₃ to Coordinated Nitric Oxide in a Binuclear Metallomacrocyclic and the Crystal Structures of

anti-[Mo(NO){HB(3,5-Me₂C₃HN₂)₃}(2,7-O₂C₁₀H₆)₂·2CHCl₃·CH₂Cl₂,
syn-[Mo(NO){HB(3,5-Me₂C₃HN₂)₃}(2,7-O₂C₁₀H₆)₂·0.67CHCl₃·2.7H₂O, and
syn-[Mo(NO){HB(3,5-Me₂C₃HN₂)₃}(2,7-O₂C₁₀H₆)₂·3(CH₃)₂CO

Ferida S. McQuillan, Hongli Chen, Thomas A. Hamor, Christopher J. Jones,* and Keith Paxton

School of Chemistry, University of Birmingham, Edgbaston, Birmingham B15 2TT, U.K.

Received June 4, 1997[⊗]

The reaction between [Mo(NO)(Tp*)I₂] {Tp*⁻ = hydrotris(3,5-dimethylpyrazol-1-yl)borate} and 2,7-dihydroxynaphthalene affords, as its major product, the binuclear complex [Mo(NO)(Tp*)(2,7-O₂C₁₀H₆)₂]. The reaction appears to proceed under kinetic control so that shorter reaction times afford the *syn*-isomer (47% yield after 40 min) while longer reaction times allow the *anti*-isomer (43% yield after 48 h) to be obtained. The molecular structures of *anti*-[Mo(NO){HB(3,5-Me₂C₃HN₂)₃}(2,7-O₂C₁₀H₆)₂·2CHCl₃·CH₂Cl₂ (**1**), *syn*-[Mo(NO){HB(3,5-Me₂C₃HN₂)₃}(2,7-O₂C₁₀H₆)₂·0.67CHCl₃·2.7H₂O (**2**) and *syn*-[Mo(NO){HB(3,5-Me₂C₃HN₂)₃}(2,7-O₂C₁₀H₆)₂·3(CH₃)₂CO (**3**) have been determined crystallographically: (**1**) C₅₀H₅₆B₂N₁₄O₆Mo₂·2CHCl₃·CH₂Cl₂, triclinic, space group P $\bar{1}$, *a* = 11.535(2) Å, *b* = 14.032(3) Å, *c* = 11.247(3) Å, α = 94.70(1)°, β = 102.30(2)°, γ = 110.31(2)°, *Z* = 1; (**2**) C₅₀H₅₆B₂N₁₄O₆Mo₂·0.67CHCl₃·2.7H₂O, monoclinic space group P2₁/m, *a* = 23.770(7) Å, *b* = 26.600(10) Å, *c* = 11.334(4) Å, β = 99.86(2)°, *Z* = 4; (**3**) C₅₀H₅₆B₂N₁₄O₆Mo₂·3C₃H₆O, triclinic, space group P $\bar{1}$, *a* = 16.929(3) Å, *b* = 17.465(4) Å, *c* = 12.739(2) Å, α = 100.06(1)°, β = 94.93(2)°, γ = 114.13(1)°, *Z* = 2. In **1** each nitric oxide ligand is hydrogen bonded [C–H 0.98, H···O 2.26, C···O 3.13(2) Å, C–H···O 147°] to a chloroform molecule which lies within a cavity in the molecule having as its base a bridging 2,7-naphthalenediyl fragment and as its sides a part of each HB(3,5-Me₂C₃HN₂)₃ ligand. No hydrogen bonding interactions with nitric oxide are apparent in the structures of **2** or **3**.

Introduction

The reactions of suitable bifunctional ligands with transition metal complexes containing two labile *cis*-ligands can lead to the formation of metallomacrocycles which may have the potential to act as host molecules. An early example of a metallomacrocyclic host is provided by the work of Maverick and co-workers who used ligands containing two linked β -diketone units to form a bimetallic host when coordinated to Cu²⁺ ions.¹ Subsequently Stephan demonstrated the formation of binuclear metallomacrocycles in reactions between [Zr(η^5 -C₅H₅)₂Me₂] and dihydroxy compounds such as 1,3-(HOCH₂)₂-C₆H₄.² More recently Fujita and co-workers have prepared binuclear metallomacrocycles in self-assembly reactions involving bipyridine ligands and square planar Pd²⁺ or Pt²⁺ complexes.³ A number of other metallomacrocycles, including higher nuclearity systems, have also been reported.⁴ In seeking to prepare new metallomacrocycles containing octahedral metal centers, we have been investigating the reactions of [Mo(NO)(Tp*)I₂] {Tp*⁻ = hydrotris(3,5-dimethylpyrazol-1-yl)borate}⁵ and [Mo(=O)(Tp*)Cl₂]⁶ with ligands containing two suitably disposed hydroxy groups.⁷ In any metallomacrocyclic complex formed, the nitric oxide, or oxo, oxygen atoms offer potential hydrogen bond acceptor sites which might interact with a hydrogen bond

donor molecule. A binuclear metallomacrocyclic complex formed in the reaction of [Mo(NO)(Tp*)I₂] with 2,7-dihydroxynaphthalene has been found to exhibit such an interaction in the solid state and contains a chloroform molecule hydrogen bonded to each coordinated nitrosyl ligand.

Hydrogen-bonding interactions can have important effects on the properties of coordination compounds. In the solid state hydrogen bonding can determine the packing arrangements adopted by metal complexes and hence their electrical, magnetic, or optical properties.⁸ In solution, specific solvation interactions such as hydrogen bonding can affect the electronic structures

- (4) (a) Stricklen, P. M.; Volcko, E. J.; Verkade, J. G. *J. Am. Chem. Soc.* **1983**, *105*, 2494. (b) Fujita, M.; Yazaki, J.; Ogura, K. *J. Am. Chem. Soc.* **1990**, *112*, 5645–5647. (c) Ruttimann, S.; Bernardinalli, G.; Williams, A. F. *Angew. Chem., Int. Ed. Engl.* **1993**, *32*, 392–394. (d) Stang, P. J.; Cao, D. H. *J. Am. Chem. Soc.* **1994**, *116*, 4981–4982. (e) Stang, P. J.; Whiteford, J. A. *Organometallics* **1994**, *13*, 3776–3777. (f) Fujita, M.; Kwon, Y. J.; Satoru, W.; Ogura, K. *J. Am. Chem. Soc.* **1994**, *116*, 1151–1152. (g) Stang, P. J.; Cao, D. H.; Saito, S.; Arif, A. M. *J. Am. Chem. Soc.* **1995**, *117*, 6273–6283. (h) Slone, R. V.; Yoon, D. I.; Calhoun, R. M.; Hupp, J. T. *J. Am. Chem. Soc.* **1995**, *117*, 11813–11814. (i) Baker, A. T.; Crass, J. C.; Maniska, M.; Craig, D. C. *Inorg. Chim. Acta* **1995**, *230*, 225–229. (j) Bilyk, A.; Harding, M. M.; Turner, P.; Hambley, T. W. *J. Chem. Soc., Dalton Trans.* **1995**, 2549–2553. (k) Fujita, M.; Satoshi, N.; Ogura, K. *J. Am. Chem. Soc.* **1995**, *117*, 1649–1650.
- (5) (a) Reynolds, S. J.; Smith, C. F.; Jones, C. J.; McCleverty, J. A.; Bower, D. C.; Templeton, J. L. *Inorg. Synth.* **1985**, *23*, 4–9. (b) McCleverty, J. A. *Chem. Soc. Rev.* **1983**, *12*, 331–360. (c) Charsley, S. M.; Jones, C. J.; McCleverty, J. A.; Neaves, B. D.; Reynolds, S. J. *Transition Met. Chem.* **1986**, *11*, 329–334.
- (6) (a) Cleland, W. E.; Barnhart, K. M.; Yamanouchi, K.; Collison, D.; Mabbs, F. E.; Ortega, R. B.; Enemark, J. H. *Inorg. Chem.* **1987**, *26*, 1017. (b) Roberts, S. A.; Young, C. G.; Kipke, C. A.; Cleland, W. E., Jr.; Yamanouchi, K.; Carducci, M. D.; Enemark, J. H. *Inorg. Chem.* **1990**, *29*, 3650–3656.

[⊗] Abstract published in *Advance ACS Abstracts*, September 1, 1997.

- (1) (a) Maverick, A. W.; Klavetter, F. E. *Inorg. Chem.* **1984**, *23*, 4130. (b) Maverick, A. W.; Buckingham, S. C.; Yao, Q.; Bradbury, J. R.; Stanley, G. G. *J. Am. Chem. Soc.* **1986**, *108*, 7430–7431.
- (2) Stephan, D. W. *Organometallics* **1990**, *9*, 2718–2723.
- (3) (a) Fujita, M.; Nagao, S.; Iida, M.; Ogata, K.; Ogura, K. *J. Am. Chem. Soc.* **1993**, *115*, 1574–1576. (b) Fujita, M.; Ogura, K. *Coord. Chem. Rev.* **1996**, *148*, 249–264.

of molecules and may lead to sufficiently large changes that solvatochromism may be observed in the electronic spectra of the solute.⁹ In such cases hydrogen-bonding interactions in solution can be quantified through a statistical analysis of solvatochromism data using models such as those provided by Kamlett and Taft¹⁰ or by Drago (unified solvent parameter approach).¹¹ However, examples of transition metal complexes where such interactions have been detected in solution and corroborated by structural studies are rare. We have recently carried out a solvatochromism study¹² of the metal to ligand charge transfer (MLCT) band in the electronic spectra of the 17-electron molybdenum mononitrosyl complexes [$\{\text{Mo}(\text{NO})(\text{Tp}^*)\text{X}\}_x(\text{L-L})$] ($\text{X} = \text{Cl, I}; x = 1, 2; \text{L-L} = 1,8\text{-bis}(4'\text{-pyridyl})\text{-octatetraene}$).¹³ This revealed that hydrogen bond-donor solvents produce hypsochromic shifts in the MLCT band; that is they stabilize the ground state of the molecule through hydrogen bonding to the complex. A comparison of the data obtained for the mono- and bimetallic chloro and iodo derivatives indicated that the nitric oxide ligand is the most probable site of hydrogen bonding leading to this effect. Although examples of C–H hydrogen bonds to coordinated carbon monoxide are now well established and the subject of a recent review,¹⁴ we are aware of only one other well-documented example of a solvent hydrogen-bonding interaction to a coordinated nitric oxide ligand.¹⁵

Experimental Section

General Details. All reactions were carried out under an oxygen-free, dry nitrogen atmosphere. Dry, freshly distilled dichloromethane or toluene was used for all reactions. Triethylamine was dried over molecular sieves (4A) and stored over activated alumina. The starting material $[\text{Mo}(\text{NO})(\text{Tp}^*)\text{I}_2] \cdot \text{C}_6\text{H}_5\text{CH}_3$ was prepared by following known procedures^{5a} as were samples of $[\text{Mo}(\text{NO})(\text{Tp}^*)\text{I}(2,7\text{-OC}_{10}\text{H}_6\text{OH})]$ and $[\{\text{Mo}(\text{NO})(\text{Tp}^*)\}_2(2,7\text{-O}_2\text{C}_{10}\text{H}_6)]$.^{5c} The new compounds were purified by column chromatography using silica gel (Merck; Kiesel gel 60, 70–230 mesh). IR spectra were recorded on a Perkin-Elmer 1600 series

FT-IR spectrophotometer from KBr disks. ¹H NMR spectra were recorded using a Bruker AMX-400 (400 MHz) spectrometer. Liquid secondary ion mass spectra (LSIMS) were obtained from a VG Zabspec mass spectrometer utilising a *m*-nitrobenzyl alcohol matrix and scanning in the positive ion mode at a speed of 5 s/decade.

Cyclic voltammetry was carried out using an EG & G model 174A polarographic analyzer, with *ca.* 10^{-3} mol·dm⁻³ solutions under dry N₂ in dry solvents. A Pt bead working electrode was used, with 0.2 mol·dm⁻³ $[\text{Bu}^n\text{N}][\text{BF}_4]$ as the supporting electrolyte and a scan rate of 200 mV s⁻¹. Potentials were recorded vs a saturated calomel reference electrode, and ferrocene was added as an internal standard. The data obtained were reproducible, the experimental error being ± 10 mV. Microanalyses were performed by the Microanalytical Laboratory of the University of North London on finely ground samples dried for several days *in vacuo* at 100 °C to remove solvent.

Preparation of *syn*-[Mo(NO)(Tp^{*})(2,7-O₂C₁₀H₆)₂]. To a solution of $[\text{Mo}(\text{NO})(\text{Tp}^*)\text{I}_2] \cdot \text{C}_6\text{H}_5\text{CH}_3$ (0.500 g, 0.650 mmol) in dry toluene (50 cm³) was added NEt₃ (0.5 cm³). The mixture was stirred for 5 min before adding 2,7-dihydroxynaphthalene (0.118 g, 0.738 mmol) and heating the mixture under reflux for 40 min. The dark brown solution was allowed to cool to room temperature and filtered. The filtrate was evaporated to dryness *in vacuo* and the residue purified by column chromatography on silica gel using a mixture of dichloromethane and *n*-hexane (1:1 v/v) as the eluant. The first major dark brown fraction to elute was collected, the solvent removed *in vacuo*, and the product obtained as dark brown crystals by recrystallization from dichloromethane/*n*-hexane.

Yield: 0.179 g (47%). ¹H NMR [400 MHz, (CD₃)₂CO]: δ 8.30 (4H, d, ⁴*J* 2.4 Hz), 7.62 (4H, d, ³*J* 8.8 Hz), 6.99 (4H, dd, ⁴*J* 2.4, ³*J* 8.8 Hz, C₁₀H₆O₂), 5.91 (4H, s), 5.80 (2H, s, Me₂C₃HN₂), 2.44 (30H, s), 2.06 {6H, s, (CH₃)₂C₃HN₂}. Anal. Found: C, 51.7; H, 4.4; N, 16.6. Calc for C₅₀H₅₆B₂N₁₄O₆Mo₂: C, 51.7; H, 4.9; N, 16.9. FAB MS: *m/z* 1163 (M⁺). IR data (KBr disk): 2927 w (ν_{CH}), 2543 w (ν_{BH}); 1664 s (ν_{NO}), 1542 m, 1498 m ($\nu_{\text{C}=\text{C}}$), 1448 s, 1418 m, 1364 s ($\nu_{\text{C}-\text{Me}}$) cm⁻¹.

Preparation of *anti*-[Mo(NO)(Tp^{*})(2,7-O₂C₁₀H₆)₂]. To a solution of $[\text{Mo}(\text{NO})(\text{Tp}^*)\text{I}_2] \cdot \text{C}_6\text{H}_5\text{CH}_3$ (0.500 g, 0.650 mmol) in dry toluene (50 cm³) was added NEt₃ (0.5 cm³). The mixture was stirred for 5 min before adding 2,7-dihydroxynaphthalene (0.118 g, 0.738 mmol) and heating the mixture under reflux for 48 h. The dark brown suspension was allowed to cool to room temperature and the brown solid collected by filtration. This product was redissolved in chloroform (30 cm³) and absorbed on the top of a silica gel chromatography column which was subsequently eluted with a mixture of dichloromethane and *n*-hexane (6:4 v/v). The first major dark brown fraction to elute was collected, the solvent removed *in vacuo*, and the product obtained as dark brown crystals by recrystallization from chloroform/dichloromethane.

Yield: 0.162 g (43%). ¹H NMR (400 MHz, CDCl₃): δ 7.91 (4H, d, ⁴*J* 2.3 Hz), 7.74 (4H, d, ³*J* 8.8 Hz), 7.10 (4H, dd, ⁴*J* 2.4, ³*J* 8.8 Hz, C₁₀H₆O₂), 5.87 (4H, s), 5.80 (2H, s, Me₂C₃HN₂), 2.45 (6H, s), 2.43 (12H, s), 2.31 (12H, s), 2.24 {6H, s, (CH₃)₂C₃HN₂}. Anal. Found: C, 51.7; H, 4.8; N, 16.8. Calc for C₅₀H₅₆B₂N₁₄O₆Mo₂: C, 51.7; H, 4.9; N, 16.9. FAB MS: *m/z* 1162 (M⁺). IR data (KBr disk): 2924 w, 2854 w (ν_{CH}), 2542 w (ν_{BH}); 1662 s (ν_{NO}), 1543 m, 1499 m ($\nu_{\text{C}-\text{C}}$), 1449 s, 1417 m, 1362 s ($\nu_{\text{C}-\text{Me}}$) cm⁻¹.

Structure Determinations.¹⁶ Data for all three structures were measured on a Rigaku R-Axis II area detector diffractometer with Mo K α radiation ($\lambda = 0.71069 \text{ \AA}$), *anti*-[Mo(NO){HB(3,5-Me₂C₃HN₂)₃}(2,7-O₂C₁₀H₆)₂·2CHCl₃·CH₂Cl₂ (**1**) and *syn*-[Mo(NO){HB(3,5-Me₂C₃HN₂)₃}(2,7-O₂C₁₀H₆)₂·0.67CHCl₃·2.7H₂O (**2**) at 293(2) K and *syn*-[Mo(NO){HB(3,5-Me₂C₃HN₂)₃}(2,7-O₂C₁₀H₆)₂·3(CH₃)₂CO (**3**) at 243(2) K (Table 1). The structures were determined by direct methods^{16a} and refined^{16b} on F² by least squares with anisotropic displacement parameters for the non-hydrogen atoms of the complexes. Hydrogen atoms were placed in calculated positions. The well-defined chloroform solvent molecules in **1** and **2** (0.67 occupancy in **2**) were

- (7) (a) Jones, C. J.; McWhinnie, S. L. W.; McQuillan, F. S.; McCleverty, J. A. In *Molecular Electrochemistry of Inorganic, Bioinorganic and Organometallic Compounds*; Pombiero, A. J. L., McCleverty, J. A., Eds.; NATO ASI Series C; Kluwer Academic Publishers: Dordrecht, The Netherlands, 1993; Vol. 385, p 89. (b) McQuillan, F. S.; Jones, C. J.; McCleverty, J. A. *Polyhedron* **1995**, *14*, 3157–3160. (c) McQuillan, F. S.; Jones, C. J. *Polyhedron* **1996**, *15*, 1553–1557. (d) McQuillan, F. S.; Chen, H.; Hamor, T. A.; Jones, C. J. *Polyhedron* **1996**, *15*, 3909–3913. (e) Berridge, T. E.; Jones, C. J. *Polyhedron* **1997**, *16*, 3695–3698.
- (8) Burrows, A. D.; Chan, C.-W.; Chowdhry, M. M.; McGrady, J. E.; Mingos, D. M. P. *Chem. Soc. Rev.* **1995**, *24*, 329 and references therein.
- (9) *Developments in the Chemistry and Technology of Organic Dyes*; Griffiths, J., Ed.; Blackwell Scientific: Oxford, U.K., 1983.
- (10) (a) Abboud, J.-L. M.; Kamlet, M. J.; Taft, R. W. *Prog. Phys. Org. Chem.* **1981**, *13*, 485. (b) Kamlet, M. J.; Abboud, J.-L. M.; Abraham, M. H.; Taft, R. W.; *J. Org. Chem.* **1983**, *48*, 2877–2887. (c) Marcus, Y. *Chem. Soc. Rev.* **1993**, *22*, 409–416.
- (11) (a) Drago, R. S. *J. Chem. Soc., Perkin Trans. 2*, **1992**, 1827–1838. (b) Drago, R. S. *J. Org. Chem.* **1992**, *57*, 6547–6552. (c) Drago, R. S.; Hirsch, M. S.; Ferris, D. C.; Chronister, C. W. *J. Chem. Soc., Perkin Trans. 2* **1994**, 219–230.
- (12) Thomas, J. A.; Hutchings, M. G.; Jones, C. J.; McCleverty, J. A. *Inorg. Chem.* **1996**, *35*, 289–296.
- (13) McWhinnie, S. L. W.; Thomas, J. A.; Hamor, T. A.; Jones, C. J.; McCleverty, J. A.; Collison, D.; Mabbs, F. E.; Harding, C. J.; Yellowlees, L. J.; Hutchings, M. G. *Inorg. Chem.* **1996**, *35*, 760–774.
- (14) Braga, D.; Grepioni, F.; Biradha, K.; Pedireddi, V. R.; Desiraju, G. R. *J. Am. Chem. Soc.* **1995**, *117*, 3156–3166.
- (15) A search of the Cambridge Crystallographic Database revealed no examples of C–H···O(N–metal) interactions with H···O distances of less than 2.35 Å involving a chloroform molecule. One example of a dichloromethane molecule interacting with a rhenium nitrosyl complex has H···O 2.17 Å and angle C–H···O 175°; O'Connor, J. M.; Uhrhammer, R.; Chadha, R. K. *Polyhedron* **1993**, *12*, 527.

- (16) (a) TeXsan: Single Crystal Analysis Software, version 1.6 (1993), Molecular Structure Corp., The Woodlands, TX 77381. (b) Sheldrick, G. M. SHELXL-93, Program for Crystal Structure Refinement, University of Göttingen, 1993. (c) Johnson, C. K. *ORTEP*; Report ORNL-5138; Oak Ridge National Laboratory: Oak Ridge, TN, 1976.

Table 1. Crystallographic Data

	1	2	3
formula	C ₅₀ H ₅₆ B ₂ N ₁₄ O ₆ Mo ₂ ·2CHCl ₃ ·CH ₂ Cl ₂	C ₅₀ H ₅₆ B ₂ N ₁₄ O ₆ Mo ₂ ·0.67CHCl ₃	C ₅₀ H ₅₆ B ₂ N ₁₄ O ₆ Mo ₂ ·2.7H ₂ O· ₃ C ₃ H ₆ O
fw	1486.3	1290.9	1336.8
a, Å	11.535(2)	23.770(7)	16.929(3)
b, Å	14.032(3)	26.600(10)	17.465(4)
c, Å	11.247(3)	11.334(4)	12.739(2)
α, deg	94.70(1)	90	100.06(1)
β, deg	102.30(2)	99.86(2)	94.93(2)
γ, deg	110.31(2)	90	114.13(1)
V, Å ³	1643.7(6)	7060(4)	3332(1)
Z	1	4	2
space grp	<i>P</i> $\bar{1}$ (No. 2)	<i>P</i> 2 ₁ / <i>m</i> (No. 11)	<i>P</i> $\bar{1}$ (No. 2)
T, °C	20	20	-50
λ, Å	0.7107	0.7107	0.7107
ρ _{calcd}	1.501	1.214	1.332
μ(Mo Kα), mm ⁻¹	0.764	0.484	0.438
R _w (F _o ²)	0.1782	0.2439	0.2120
R(F _o) for obsd rflns ^a	0.0660	0.0692	0.0809

$$^a R_w(F_o^2) = [\sum w(F_o^2 - F_c^2)^2 / \sum w(F_o^2)^2]^{1/2}. R(F_o) = \sum (|F_o - F_c|) / \sum |F_o|.$$

treated likewise. The disordered carbon atoms of the dichloromethane solvent molecule (0.5 occupancy) in **1** and water molecules in **2** (site occupancies 0.25–0.5) were treated isotropically, as were the acetone molecules in **3**, one of which is disordered and ill-defined. The figures were drawn using ORTEP.^{16c}

Results and Discussion

Synthetic Studies. The reaction between [Mo(NO)(Tp*)I₂] and 2,7-dihydroxynaphthalene affords, as its major product, the binuclear complex [Mo(NO)(Tp*)(2,7-O₂C₁₀H₆)₂] which exists in either of two isomeric forms, one with the two nitrosyl ligands oriented *syn* and the other *anti* with respect to the macrocyclic ring plane. The reaction appears to proceed under kinetic control so that it is possible to obtain these isomers selectively by using different reaction conditions. Short reaction times afford mainly the *syn*-isomer while longer reaction times allow the *anti*-isomer to be obtained. Thus *syn*-[Mo(NO)(Tp*)(2,7-O₂C₁₀H₆)₂] may be prepared in 43% yield from the reaction between [Mo(NO)(Tp*)I₂] and 2,7-dihydroxynaphthalene in toluene containing NEt₃ when a reaction time of 40 min under reflux is used. If instead the reaction is allowed to proceed for 48 h the toluene-insoluble *anti*-isomer is precipitated and may be isolated in 47% yield. The purified isomers cannot be interconverted by heating under reflux in toluene for 48 h so it appears that the metallomacrocycle formation reaction does not proceed under equilibrium control and does not, therefore, constitute an example of self-assembly. The two isomers differ substantially in solubility. The *syn*-isomer is soluble in polar organic solvents such as dichloromethane, acetone, and tetrahydrofuran, but the *anti*-isomer is sparingly soluble, if at all, in these solvents. However, the *anti*-isomer is freely soluble in chloroform, as is the *syn*-isomer. The infrared and ¹H NMR spectra of the two compounds are in accord with their formulations, and the latter reflect the presence of a putative symmetry plane in each molecule when in solution. The mass spectra of the two isomers are similar, exhibiting ion clusters based at *m/z* 1162 (*anti*-isomer) or 1163 (*syn*-isomer) in accord with the presence of the cyclic dimer. Ions attributable to higher cyclic oligomers were absent from the purified samples, although mass spectrometric data do indicate the presence of small quantities of cyclic trimers and tetramers in solutions of the crude reaction mixture. The mechanism of formation of the cyclic dimers remains unclear. Three pathways are possible, and any or all of these may be operating. The first involves monosubstitution of [Mo(NO)(Tp*)I₂] to afford a racemic mixture containing the two chiral forms of the complex [Mo(NO)(Tp*)(2,7-O₂C₁₀H₆)I]. Two molecules of this compound may then react together to

form the cyclic dimer [Mo(NO)(Tp*)(2,7-O₂C₁₀H₆)₂]. Where molecules of like chirality react, the *syn*-isomer will be formed, and where molecules of opposite chirality react, the *anti*-isomer will be formed. The second pathway involves addition of a further metal center to [Mo(NO)(Tp*)(2,7-O₂C₁₀H₆)I] forming a mixture of *meso*- and *dl*-isomers of the bimetallic complex [{Mo(NO)(Tp*)I}₂(2,7-O₂C₁₀H₆)]. Reaction of this complex with further dihydroxynaphthalene then affords the cyclic dimer, the *meso*-complex giving rise to the *syn*-isomer and the *dl*-complex the *anti*-isomer. The third pathway involves prior formation of the achiral bis-substituted complex [Mo(NO)(Tp*)(2,7-O₂C₁₀H₆)₂] followed by reaction with a further molecule of [Mo(NO)(Tp*)I₂] to give a mixture of the isomers of the cyclic dimer. In an attempt to demonstrate which of these reaction pathways might be viable, samples of [Mo(NO)(Tp*)(2,7-OC₁₀H₆OH)I] and [{Mo(NO)(Tp*)I}₂(2,7-O₂C₁₀H₆)] were prepared. However, attempts to obtain pure samples of [Mo(NO)(Tp*)(2,7-OC₁₀H₆OH)₂] for reaction with [Mo(NO)(Tp*)I₂] have been unsuccessful. Treatment of a solution of *rac*-[Mo(NO)(Tp*)(2,7-OC₁₀H₆OH)I] in toluene with triethylamine affords a mixture of products including the binuclear metallomacrocycles [Mo(NO)(Tp*)(2,7-O₂C₁₀H₆)₂]. The reaction of a mixture of *meso*- and *dl*-[{Mo(NO)(Tp*)I}₂(2,7-O₂C₁₀H₆)] with further 2,7-dihydroxynaphthalene also affords [Mo(NO)(Tp*)(2,7-O₂C₁₀H₆)₂]. However, in this case a more complex mixture of products is obtained so that this approach provides a less efficient route to the bimetallo-macrocycles. Thus it seems that these two pathways, at least, could be involved in the formation of *syn*- and *anti*-[Mo(NO)(Tp*)(2,7-O₂C₁₀H₆)₂] and more than one reaction pathway is probably involved. Because the syntheses of [Mo(NO)(Tp*)I(2,7-OC₁₀H₆OH)] and [{Mo(NO)(Tp*)I}₂(2,7-O₂C₁₀H₆)] do not proceed in high yield, the single step reaction between [Mo(NO)(Tp*)I₂] and 2,7-dihydroxynaphthalene constitutes the most efficient synthetic route to the binuclear metallomacro-cycles.

Electrochemical Studies. Because of its poor solubility in other solvents, attempts were made to obtain the cyclic voltammogram of *anti*-[Mo(NO)(Tp*)(2,7-O₂C₁₀H₆)₂] in CHCl₃ solution. However, this solvent appeared to be reactive at reduction potentials less negative than those of the complex and no meaningful electrochemical data could be obtained. The cyclic voltammogram of a dichloromethane solution of *syn*-[Mo(NO)(Tp*)(2,7-O₂C₁₀H₆)₂] contained two reversible waves at *E*_f = -0.633 (Δ*E*_p = 77 mV) and -0.807 V (Δ*E*_p = 86 mV) (*E*_f vs SCE; internal standard Fc/Fc⁺, *E*_f = 0.546, Δ*E*_p =

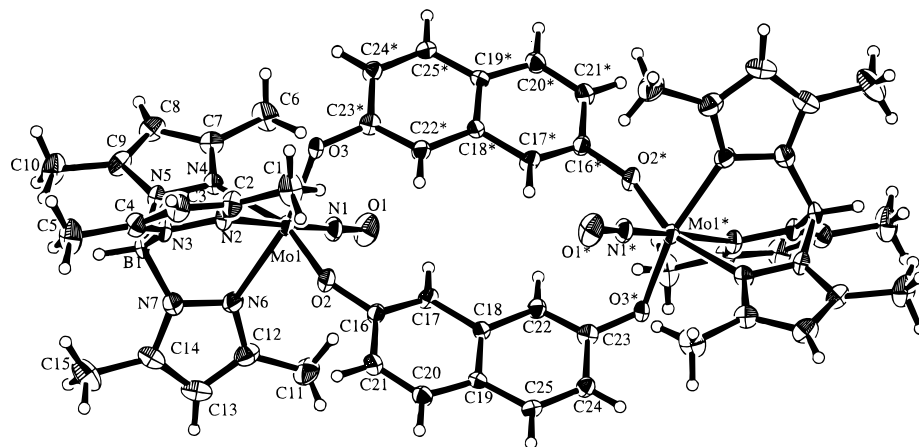


Figure 1. View of complex **1** in a direction approximately perpendicular to the central near-planar group of atoms O(2), O(3), O(2)*, and O(3)* and the adjoining carbon atoms of the naphthalene residues. Ellipsoids are drawn at the 33% probability level. Starred atoms are related to the corresponding unstarred atoms by an inversion center.

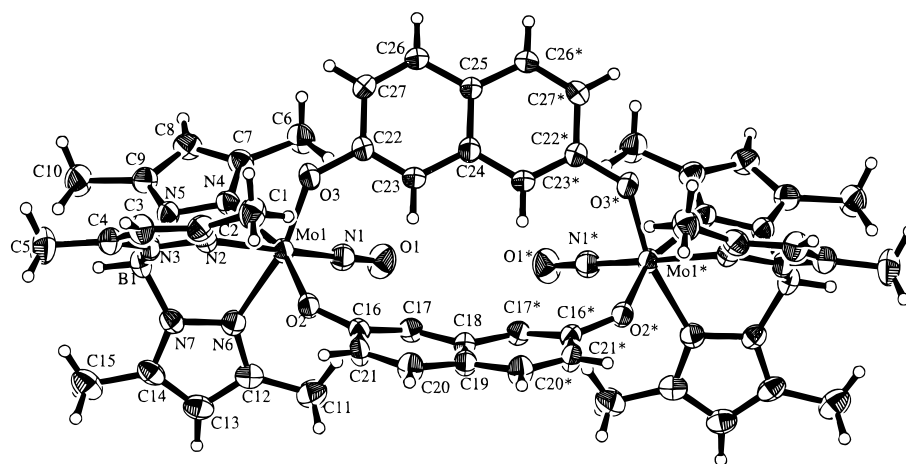


Figure 2. View of complex **2** (molecule A) with view direction as for **1**. Starred atoms are related to the corresponding unstarred atoms by a mirror plane. Molecule B is similar and is not shown.

76 mV). These reduction potentials lie on either side of the reduction potential of -0.74 V reported^{17a} for $[\text{Mo}(\text{NO})(\text{Tp}^*)(\text{OPh})_2]$, and the separation (ΔE_f) of 174 mV between the first and second reduction potentials of *syn*- $[\text{Mo}(\text{NO})(\text{Tp}^*)(2,7\text{-O}_2\text{C}_{10}\text{H}_6)_2]$ is slightly larger than that of 150 mV found^{17b} for the corresponding acyclic binuclear complex $[\{\text{Mo}(\text{NO})(\text{Tp}^*)\text{Cl}\}_2(2,7\text{-O}_2\text{C}_{10}\text{H}_6)]$. In contrast to this finding, the successive ΔE_f values of 420 and 320 mV for the three reduction potentials of *syn*, *syn*- $[\text{Mo}(\text{NO})(\text{Tp}^*)(1,4\text{-O}_2\text{C}_6\text{H}_4)]_3$ ^{7d} are slightly smaller than the value of 460 mV found in the binuclear acyclic complex $[\{\text{Mo}(\text{NO})(\text{Tp}^*)\text{Cl}\}_2(1,4\text{-O}_2\text{C}_6\text{H}_4)]$.^{17c} This suggests that, in these metallomacrocycles, ΔE_f values may be affected by geometric factors as well as electrostatic effects and ligand-mediated metal–metal interactions. This might be expected since the Mo–S–C–C(aryl) torsion angles in $[\text{Mo}(\eta^5\text{-C}_5\text{H}_5)(\text{NO})(\text{SPh})_2]$ have been shown^{17d} to affect the energy of the LUMO of this complex. Furthermore, in $[\text{Mo}(\text{NO})(\text{Tp}^*)(1,2\text{-S}_2\text{C}_6\text{H}_3\text{Me-3})]$ the reduction potential is shifted in the positive direction compared to $[\text{Mo}(\text{NO})(\text{Tp}^*)(\text{SPh})_2]$,^{17e} again reflecting

the effect of the Mo–S–C–C(aryl) torsion angles on the energy of the redox orbital. Thus it seems reasonable to assume that, where the geometric constraints imposed by forming the macrocyclic ring impinge on the Mo–O–C–C(aryl) torsion angles, the reduction potentials of the metallomacrocyclic will be also be subject to geometric effects.

Structural Studies. Single-crystal X-ray diffraction studies were carried out on crystals of the *syn*- and *anti*-isomers grown from chloroform/dichloromethane solutions and of the *syn*-isomer grown from acetone solution. The structures of the *anti*-complex in crystals of *anti*- $[\text{Mo}(\text{NO})\{\text{HB}(3,5\text{-Me}_2\text{C}_3\text{HN}_2)_3\}(2,7\text{-O}_2\text{C}_{10}\text{H}_6)_2 \cdot 2\text{CHCl}_3 \cdot \text{CH}_2\text{Cl}_2$ (**1**) and the *syn*-complex in *syn*- $[\text{Mo}(\text{NO})\{\text{HB}(3,5\text{-Me}_2\text{C}_3\text{HN}_2)_3\}(2,7\text{-O}_2\text{C}_{10}\text{H}_6)_2 \cdot 0.67\text{CHCl}_3 \cdot 2.7\text{H}_2\text{O}$ (**2**) and *syn*- $[\text{Mo}(\text{NO})\{\text{HB}(3,5\text{-Me}_2\text{C}_3\text{HN}_2)_3\}(2,7\text{-O}_2\text{C}_{10}\text{H}_6)_2 \cdot 3(\text{CH}_3)_2\text{CO}$ (**3**) have been determined. The *anti*-complex is centrosymmetric. In **2** there are two independent complex molecules in the unit cell, each of which has crystallographic mirror symmetry. In the acetone solvate (**3**), the *syn*-complex has no crystallographic symmetry but approximates to mirror symmetry. Views of the three complexes are shown in Figures 1–3, and selected geometric parameters are presented in Table 2.

The coordination geometry at the molybdenum atoms is approximately octahedral in each case. The maximum angular distortions from ideal octahedral occur at the *trans*-angles N(4)–Mo–O(2) and N(6)–Mo–O(3) which are in the range 159.3–166.5°. The mean deviations from ideal octahedral are within

(17) (a) Obaidi, N. A.; Chaudhury, M.; Clague, D.; Jones, C. J.; Pearson, J. C.; McCleverty, J. A.; Salam, S. S. *J. Chem. Soc., Dalton Trans.* **1987**, 1733–1736. (b) Charsley, S. M.; Jones, C. J.; McCleverty, J. A. *Transition Met. Chem.* **1986**, *11*, 329–334. (c) Charsley, S. M.; Jones, C. J.; McCleverty, J. A.; Neaves, B. D.; Reynolds, S. J.; Denti, G. *J. Chem. Soc., Dalton Trans.* **1988**, 293–299. (d) Ashby, M. T.; Enemark, J. H. *J. Am. Chem. Soc.* **1986**, *108*, 708–733. (e) Obaidi, N. A.; Jones, C. J.; McCleverty, J. A. *Polyhedron* **1989**, *8*, 1033–1037.

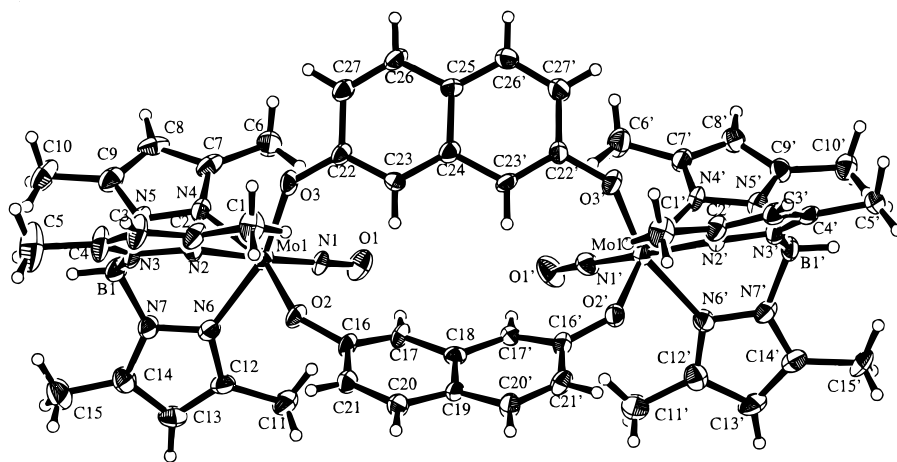


Figure 3. View of complex **3** with view direction as for **1**. Primed atoms are related to the corresponding unprimed atoms by an approximate (noncrystallographic) mirror plane.

Table 2. Selected Structural Parameters for **1–3**^{a,b}

	1	2		3	
		molecule A	molecule B	Mo	Mo'
Distances (Å)					
Mo–N(1)	1.752(7)	1.749(6)	1.768(6)	1.756(10)	1.749(11)
Mo–N(2)	2.244(6)	2.223(5)	2.239(5)	2.222(10)	2.232(10)
Mo–N(4)	2.202(5)	2.188(5)	2.200(6)	2.173(10)	2.192(10)
Mo–N(6)	2.200(7)	2.179(5)	2.173(6)	2.165(10)	2.169(10)
Mo–O(2)	1.926(5)	1.956(5)	1.960(5)	1.945(10)	1.945(10)
Mo–O(3)	1.973(5)	1.942(5)	1.964(5)	1.940(10)	1.943(10)
N(1)–O(1)	1.200(8)	1.208(7)	1.195(7)	1.213(10)	1.233(12)
O(2)–C(16)	1.352(8)	1.352(7)	1.340(8)	1.363(12)	1.364(12)
O(3)–C*	1.359(9)	1.360(7)	1.363(8)	1.337(12)	1.373(12)
Angles (deg)					
N(1)–Mo–N(2)	178.1(3)	177.3(2)	178.2(3)	177.8(4)	176.8(4)
N(1)–Mo–N(4)	94.4(3)	93.8(2)	93.6(3)	94.9(4)	91.1(4)
N(1)–Mo–N(6)	94.3(3)	93.5(2)	94.8(3)	96.2(4)	96.0(4)
N(1)–Mo–O(2)	98.6(3)	99.7(2)	98.8(3)	98.5(4)	98.2(4)
N(1)–Mo–O(3)	95.3(3)	95.5(2)	96.8(3)	96.1(4)	98.2(4)
N(2)–Mo–N(4)	83.9(2)	83.6(2)	84.7(2)	84.5(4)	85.8(3)
N(2)–Mo–N(6)	86.1(2)	86.1(2)	84.5(2)	85.7(3)	82.9(4)
N(2)–Mo–O(2)	83.2(2)	82.9(2)	82.8(2)	82.6(3)	84.8(3)
N(2)–Mo–O(3)	84.0(2)	84.4(2)	83.5(2)	81.8(3)	82.2(3)
N(4)–Mo–N(6)	77.4(2)	78.4(2)	78.0(3)	77.8(4)	79.1(4)
N(4)–Mo–O(2)	159.3(2)	161.8(2)	162.6(2)	161.2(3)	165.1(3)
N(4)–Mo–O(3)	92.5(2)	90.7(2)	89.0(2)	89.2(3)	89.2(3)
N(6)–Mo–O(2)	85.6(2)	88.7(2)	88.8(2)	87.6(4)	88.3(3)
N(6)–Mo–O(3)	166.5(2)	166.2(2)	163.1(2)	162.8(3)	161.6(3)
O(2)–Mo–O(3)	102.1(2)	100.0(2)	101.5(2)	102.3(3)	101.0(3)
Mo–N(1)–O(1)	178.0(7)	177.5(6)	177.5(6)	179.4(8)	177.1(9)
Mo–O(2)–C(16)	141.6(5)	138.2(4)	137.8(4)	140.7(7)	136.6(7)
Mo–O(3)–C*	125.8(5)	130.1(4)	129.6(4)	132.0(7)	134.1(7)
Torsion Angles (deg)					
N(1)–Mo–O(2)–C(16)	4.8(8)	22.6(7)	23.3(7)	16.1(12)	–22.3(11)
N(1)–Mo–O(3)–C*	–23.1(5)	–13.8(6)	–13.0(6)	–21.5(10)	14.0(11)

^a Values in parentheses are estimated standard deviations. ^b C* is C(23) in **1** and C(22) in **2** and **3**.

a fairly narrow range, from 6.9° in molecule **A** of structure **2** to 7.8° in structure **3**. These values are at the upper end of the range commonly found in monomeric species, e.g. 7.1° in [Mo(NO)Tp*(NH-Py)₂]₂,^{18a} 6.5 and 5.9° in the two independent molecules in the crystal structure of [Mo(NO)(Tp*)Cl(OC₆H₄-CH=CH-C₆H₄NMe₂)₂]₂,^{18b} and 5.6° in 5-[p-[Mo(NO)(Tp*)Cl(OC₆H₄)-10,15,20-Ph₃porphH₂]₂]^{18c} (C₆H₄-10,15,20-Ph₃porphH₂

= tetraphenylporphyrinyl). These deviations, however, show a consistent pattern. Thus the mean difference between corresponding angles at the five molybdenum centers in the present study (Table 2) are relatively small, 0.8–2.5°. Comparison of these molybdenum centers with the monomeric [Mo(NO)(Tp*)-(NH-Py)₂]₂^{18a} shows that the mean differences are of similar magnitude, 0.85–1.6°.

The molybdenum–nitrosyl moieties are near-linear, Mo–N–O angles 177.1–179.4, mean 177.9(4)°, with short Mo–N bonds, mean 1.755(4) Å, and relatively long Mo–N(pyrazolyl) bonds trans to these, mean 2.232(4) Å. The other Mo–N(pyrazolyl) bonds are somewhat shorter, mean 2.184(4) Å. These values are again similar to those found in monomeric

(18) (a) Obaidi, N. A.; Hamor, T. A.; Jones, C. J.; McCleverty, J. A.; Paxton, K. *J. Chem. Soc., Dalton Trans.* **1987**, 1063–1069. (b) Coe, B. J.; Hamor, T. A.; Jones, C. J.; McCleverty, J. A.; Bloor, D.; Cross, G. H.; Axon, T. L. *J. Chem. Soc., Dalton Trans.* **1995**, 673–684. (c) Rowley, N. M.; Kurek, S. S.; Foulon, J.-D.; Hamor, T. A.; Jones, J. J. (d) McCleverty, J. A.; Hubig, S. M.; McInnes, E. J. L.; Payne, N. N.; Yellowlees, L. *J. Inorg. Chem.* **1995**, *34*, 4414–4426.

analogues.^{18a-c} The lengthening of the Mo–N(pyrazolyl) bond trans to NO, relative to those trans to ligands such as oxygen, nitrogen, or halogen, has been attributed¹⁹ to the trans influence of the strongly π -accepting nitrosyl group.

In both the *anti*- and the *syn*-complexes, the Mo–O(naphthyl) bonds are relatively short, 1.926 and 1.973 Å in the *anti*-complex and 1.940–1.964, mean 1.949(3) Å, in the *syn*-complexes. This is consistent with $p\pi-d\pi$ electron donation from the donor atom (O) to the coordinatively unsaturated molybdenum. Large Mo–O–C angles, 125.8 and 141.6° in the *anti* complex and 129.6–140.7°, mean 134.9(14)°, in the *syn*-complexes, and generally small N(nitrosyl)–Mo–O–C(naphthyl) torsion angles ($<\pm 23.5^\circ$) are also consistent with this. It may be noted that the shortest Mo–O length, Mo–O(2) in the *anti* complex, is associated with the largest Mo–O–C angle (141.6°) and the smallest ON–Mo–O–C torsion angle (4.8°). In two analogous oxido complexes,^{18b,c} Mo–O distances average 1.930(9) Å and the angles at oxygen average 131.6(6)°.

The overall conformations of the complexes can be compared by reference to a central near-planar 8-atom grouping consisting of the four oxygen atoms, O(2), O(3), O(2)*, O(3)*, and the adjoining carbon atoms of the naphthalene residues. The molybdenum atoms are displaced from this plane by distances ranging from 0.99 Å in the *anti*-complex to 1.22 Å in molecule A of the *syn*-complex (2), displacements being on opposite sides of this plane in the *anti* complex and on the same side in the *syn*-complexes. In the *anti*-complex the naphthalene rings are parallel and tilted at an angle of 24.9(2)° to the central plane. However, in the *syn*-complexes, one naphthalene ring, C(16), C(16)*, ..., C(21), C(21)* in Figures 2 and 3, is tilted more steeply with respect to the central plane at angles ranging from 45.6(2)° in 3 to 57.5(1)° in molecule A of structure 2, whereas the other naphthalene, C(22), C(22)*, ..., C(27), C(27)* in Figures 2 and 3 is almost parallel to the central 8-atom plane (tilt angle $< 5^\circ$). The former naphthalene ring systems deviate significantly from planarity, the phenyl rings being inclined at an average angle of 11.3(7)° to one another, so that the naphthalene system is bent about the central C(18)–C(19) bond. The bonded oxygen atoms deviate from the planes of their respective phenyl rings by closely similar distances in each case, average 0.286(2) Å. In each case, these deviations are in a direction such as to favour the steric requirements of forming the –Mo–O–naphthyl–O–Mo–O–naphthyl–O– central ring system. Examples in the literature of sterically crowded naphthalenes bent or twisted by similar or greater amounts are numerous and include heptahelicene,^{20a} and the octachloro,^{20b} octamethyl,^{20c} heptachloro-7-(dichloromethyl),^{20d} 1,8-diferrocenyl,^{20e} 1,8-diruthenocenyl,^{20f} and 1,8-bis(trimethylsilyl)^{20g} naphthalene derivatives. *Ab initio* calculations²¹ at the RHF 3-21G level show that the energy required to bend 2,7-dihydroxynaphthalene through the maximum angle observed (12.6°) is 15.3 kJ mol⁻¹ and to displace the two oxygen atoms by 0.29 Å from their phenyl planes is 15.1 kJ mol⁻¹, so that

the total energy requirement is relatively small, 30.4 kJ mol⁻¹. In contrast, the other naphthalene ring systems in the *syn*-complexes have normal, planar geometry, presumably related to their different orientation to the central plane. In the *anti*-complex, both the naphthalenes have their phenyl rings inclined by 7.5(4)° to one another.

The nitrogen and oxygen atoms of the nitrosyl ligands are displaced by, respectively, 2.26–2.34 Å, mean 2.31(1) Å, and 3.09–3.23 Å, mean 3.15(2) Å, from the central 8-atom plane. In the *syn*-isomers the nitrosyl ligands block off one face of the central cavity, preventing approach of guest molecules from that direction; NO...ON distances are 3.76 and 4.08 Å in molecules A and B in 2 and 4.27 Å in 3. In the *anti*-isomer both faces of the cavity are largely blocked off by the nitrosyl ligands. The cavity itself is, however, too small to accommodate even quite small guest entities. Short crossing interatomic distances in the *syn*-complexes include C(17)...C(23), C(17)...H(23), and H(17)...H(23), 3.44, 2.53, and 2.49 Å (molecule A of 2) and 3.45, 2.55, and 2.45 Å (molecule B of 2), together with the mirror-related distances. In structure 3, the corresponding distances average 3.43(1), 2.52(1), and 2.33 Å, respectively. In the *anti*-isomer (1), short crossing distances are C(17)...C(22)* 3.34, C17...H(22)* 2.75, C(22)...H(17)* 2.78, and H(17)...H(22)* 2.42 Å, together with the centrosymmetrically related distances.

Although both the *syn*-isomer crystals contain solvent of crystallization involving considerable disordering, no significant interactions with the complex molecules appear to occur. However in the *anti*-isomer, in addition to a noninteracting, disordered dichloromethane solvent molecule, two symmetry-related chloroform molecules form hydrogen bonds to the complex through the nitrosyl groups (see Figure 4). The pertinent parameters (hydrogen in calculated position) are C–H 0.98, C...O 3.13(2), H...O 2.26 Å, angle C–H...O 147°, in good agreement with previous results for C–H...O hydrogen bonds.^{22,23} The angle N–O...H is 167°, so that the hydrogen atom points in a direction close to the probable position of the oxygen lone pair electrons. Interestingly, although the chloroform molecules lie well above and below the central cavity of the complex, they seem to lie within outer cavities formed by the pyrazolyl rings of the Tp* ligands.

Evidence for the interaction between CHCl₃ and the nitrosyl group of *anti*-[Mo(NO)(Tp*)(2,7-O₂C₁₀H₆)₂]₂ was sought using infrared spectroscopy. A freshly prepared sample of *anti*-[Mo(NO)(Tp*)(2,7-O₂C₁₀H₆)₂]₂ which had not been exposed to chloroform exhibited an absorption band $\nu_{\max}(\text{NO})$ at 1662 cm⁻¹ in the solid state (KBr disk) but after crystallization from chloroform/dichloromethane $\nu_{\max}(\text{NO})$ was hypsochromically shifted by 8 cm⁻¹ to 1670 cm⁻¹. Solid samples of *syn*-[Mo(NO)(Tp*)(2,7-O₂C₁₀H₆)₂]₂ crystallized from solutions in chloroform, dichloromethane, and acetone showed smaller differences exhibiting respective $\nu_{\max}(\text{NO})$ (KBr disk) values of 1668, 1664, and 1665 cm⁻¹. The low solubility of the *anti*-isomer in solvents other than chloroform has restricted opportunities for solution studies. However, the finding that the *syn*-isomer is soluble in several polar organic solvents whereas the *anti*-isomer is soluble only in chloroform suggests that a specific solvation interaction is occurring in this case.

The energies of C–H...O hydrogen bonds have been quoted²³ as being in the range –5 to –10 kJ mol⁻¹. This lies near to

- (19) McCleverty, J. A.; Rae, A. E.; Wolochowicz, I.; Bailey, N. A.; Smith, J. M. *J. Chem. Soc., Dalton Trans.* **1982**, 429–438.
 (20) (a) Joly, M.; Defay, N.; Martin, R. H.; Declercq, J. P.; Germain, G.; Soubrier-Payen, B.; van Meerssche, M. *Helv. Chim. Acta* **1977**, *60*, 537–560. (b) Herstein, F. H. *Acta Crystallogr.* **1979**, *B35*, 1661–1670. (c) Sim, G. A. *Acta Crystallogr.* **1982**, *B38*, 623–625. (d) Carilla, J.; Fajari, L.; Garcia, R.; Julia, L.; Marcos, C.; Riera, J.; Whitaker, C. R.; Rius, J.; Aleman, C. *J. Org. Chem.* **1995**, *60*, 2721–2725. (e) Lee, M.-T.; Foxman, B. M.; Rosenblum, M. *Organometallics* **1985**, *4*, 539–547. (f) Arnold, R.; Foxman, B. M.; Rosenblum, M.; Euler, W. B. *Organometallics* **1988**, *7*, 1253–1259. (g) Sooriyakumaran, R.; Boudjouk, P.; Garvey, R. G. *Acta Crystallogr.* **1985**, *C41*, 1348–1350.
 (21) SPARTAN 4.0, Wavefunction, Inc., 18401 Von Karman, Suite 370, Irvine, CA 92715.

- (22) (a) Hamilton, W. C.; Ibers, J. A. *Hydrogen Bonding in Solids*; W. A. Benjamin, Inc., New York, 1968; pp 182–183. (b) Taylor, R.; Kennard, O. *J. Am. Chem. Soc.* **1982**, *104*, 5063–5070.
 (23) (a) Desiraju, G. R. *Acc. Chem. Res.* **1991**, *24*, 290–296. (b) Steiner, T. *J. Chem. Soc., Chem. Commun.* **1997**, 727–734.

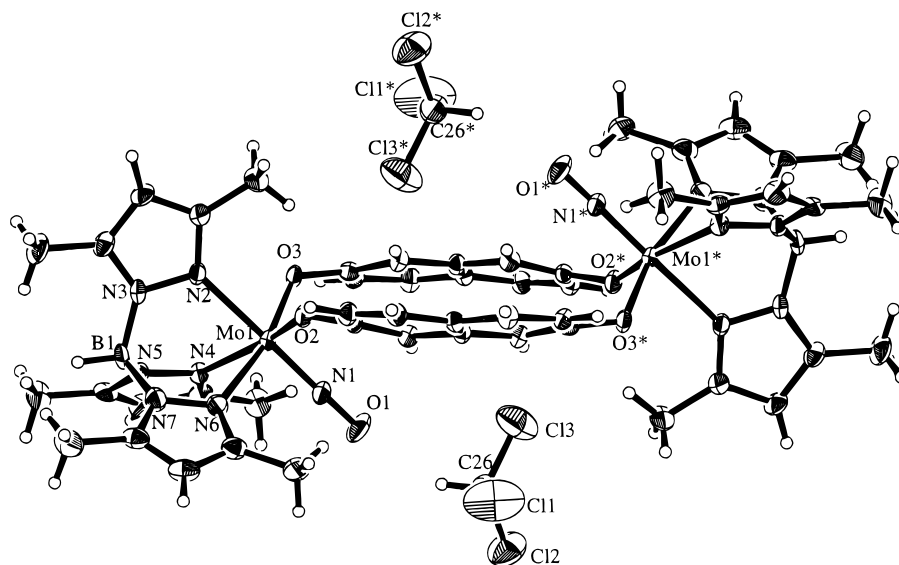


Figure 4. View of complex **1** showing the hydrogen-bonded chloroform molecules. The view direction is rotated by 65° about the Mo–Mo* axis of the molecule from that depicted in Figure 1.

the lower end of the range of values reported²⁴ for other hydrogen bonding interactions *e.g.* HCN \cdots HCN (-12 kJ mol $^{-1}$), H $_2$ O \cdots HOH (ice) (-25 kJ mol $^{-1}$), and FH \cdots F $^-$ (-161 kJ mol $^{-1}$). The low-energy electronic spectral absorption bands of the 17-electron complexes $[\{\text{Mo}(\text{NO})(\text{Tp}^*)\text{Cl}\}_x(\text{L-L})]$ (L-L = bis(4-pyridyl)octatetraene) exhibit hypsochromic shifts of 1135 ($x = 1$) and 1223 cm $^{-1}$ ($x = 2$) on changing the solvent from CCl $_4$ to CHCl $_3$.¹² Not all of these energy differences can be attributed to hydrogen bonding to NO in the ground state. An analysis of the data using the Kamlett–Taft model reveals that respective differences between the values of the solvent polarity term $c_1\pi^*$ and the hydrogen bond donor term $c_3\alpha$ for solutions in CCl $_4$ and CHCl $_3$ are, for $x = 1$, 636 and 197 cm $^{-1}$ and, for $x = 2$, 600 and 223 cm $^{-1}$.¹² This suggests that about one-fourth of this energy difference may be attributed to the effects of hydrogen bonding. This implies that, on excitation, the energy change in the chloroform to nitric oxide hydrogen bonding amounts to about 3.4 ($x = 1$) and 3.7 ($x = 2$) kJ mol $^{-1}$. These figures lie close the lower end of the suggested energy range for CH \cdots O interactions and represent the minimum energies of the Cl $_3$ CH \cdots ON interaction assuming that there is no residual hydrogen bond stabilization through nitric oxide for the excited state. The 16-electron complex $[\text{Mo}(\text{NO})(\text{Tp}^*)(2,7-$

O $_2$ C $_{10}$ H $_6$)] $_2$ would be expected to have lower electron density on the nitric oxide ligand compared to these 17-electron systems. This expectation is borne out by its higher N–O stretching frequency (1662 cm $^{-1}$) compared to values for $[\{\text{Mo}(\text{NO})(\text{Tp}^*)\text{Cl}\}_x(\text{L-L})]$ of 1595 ($x = 1$) and 1600 ($x = 2$) cm $^{-1}$. The observation of a hydrogen-bonding interaction in the solid-state structure of $[\text{Mo}(\text{NO})(\text{Tp}^*)(2,7-\text{O}_2\text{C}_{10}\text{H}_6)]_2$ lends support to the proposed specific solvation interaction in the related compounds $[\{\text{Mo}(\text{NO})(\text{Tp}^*)\text{Cl}\}_x(\text{L-L})]$ and demonstrates the potential importance of structural studies of solvent inclusion for illuminating solvation phenomena.

Acknowledgment. We are grateful to Dr. N. Spencer and Mr. M. Tolley for NMR spectroscopic measurements and to the EPSRC for supporting this work (F.S.McQ.) on Grant GR/J87572. We also thank the EPSRC and the University of Birmingham for funds to purchase the R-Axis II diffractometer and the British Council for a Sino-British Friendship Scholarship to H.C.

Supporting Information Available: X-ray crystallographic files, in CIF format, for the structures of *anti*- $[\text{Mo}(\text{NO})\{\text{HB}(3,5-\text{Me}_2\text{C}_3\text{HN}_2)_3\}(2,7-\text{O}_2\text{C}_{10}\text{H}_6)]_2 \cdot 2\text{CHCl}_3 \cdot \text{CH}_2\text{Cl}_2$, *syn*- $[\text{Mo}(\text{NO})\{\text{HB}(3,5-\text{Me}_2\text{C}_3\text{HN}_2)_3\}(2,7-\text{O}_2\text{C}_{10}\text{H}_6)]_2 \cdot 0.67\text{CHCl}_3 \cdot 2.7\text{H}_2\text{O}$, and *syn*- $[\text{Mo}(\text{NO})\{\text{HB}(3,5-\text{Me}_2\text{C}_3\text{HN}_2)_3\}(2,7-\text{O}_2\text{C}_{10}\text{H}_6)]_2 \cdot 3(\text{CH}_3)_2\text{CO}$ are available on the Internet only. Access information is given on any current masthead page.

(24) Lias, S. G.; Bartmess, J. E.; Liebman, J. F.; Holmes, J. L.; Levin, R. D.; Mallard, W. G. *J. Phys. Chem., Ref. Data*, **1988**, *17*, Suppl. 1.